Supplemental Information for "Submesoscales enhance storm-driven vertical mixing of nutrients: insights from a biogeochemical large eddy simulation"

D. B. Whitt

National Center for Atmospheric Research, Boulder, CO, USA.

M. Lévy

Sorbonne Université CNRS/IRD/MNHN, LOCEAN-IPSL, Paris, France.

J. R. Taylor

Department of Applied Mathematics and Theoretical Physics, Centre for Mathematical Sciences, University of Cambridge, Cambridge, United Kingdom.

Supplemental Figures

This section includes a series of supplemental figures, primarily to illustrate the results of the sensitivity experiments with weaker winds. Table 1 in the main manuscript lists all the simulations. The references to other figures in the captions here in the supplemental material are also to other figures here in the supplemental material—not the figures in the main text—unless otherwise noted.

*Corresponding author: D. B. Whitt, National Center for Atmospheric Research, PO Box 3000, Boulder, CO 80307, USA. (dwhitt@ucar.edu)

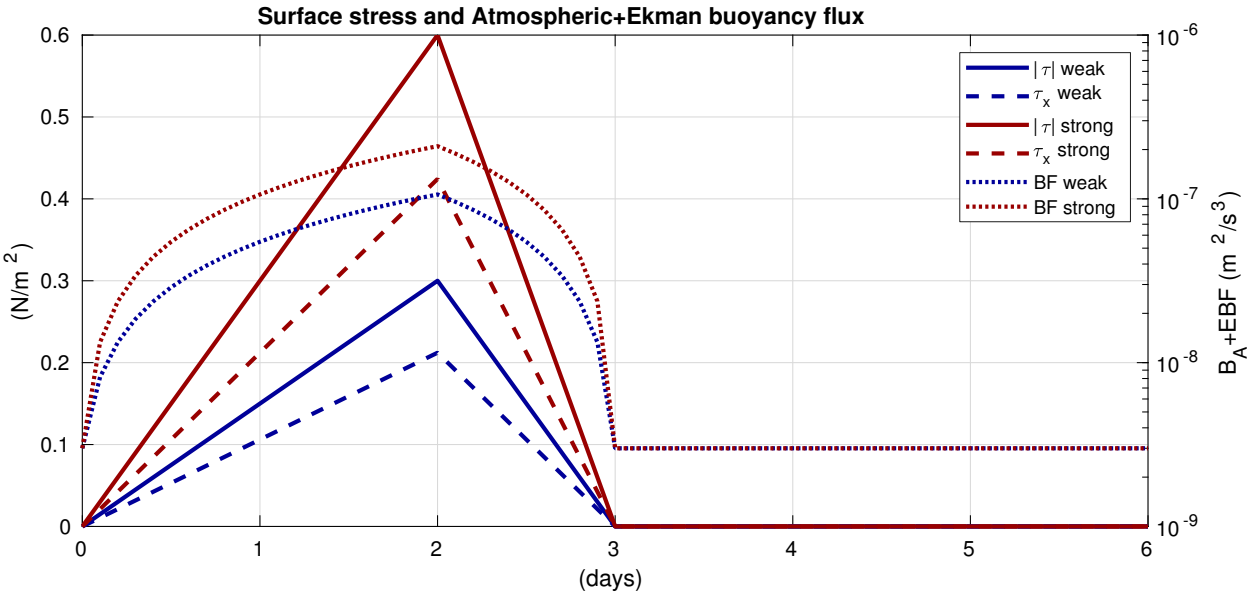

Figure 1: Time series of the magnitude of the surface stress (solid lines), which is directed to the southeast 45° to the right of the mean geostrophic flow at the surface in both scenarios. The atmospheric and Ekman buoyancy flux B_A+EBF, where $B_A = 3 \times 10^{-9}$ m^2/s^3 is constant, is indicated by dashed lines.

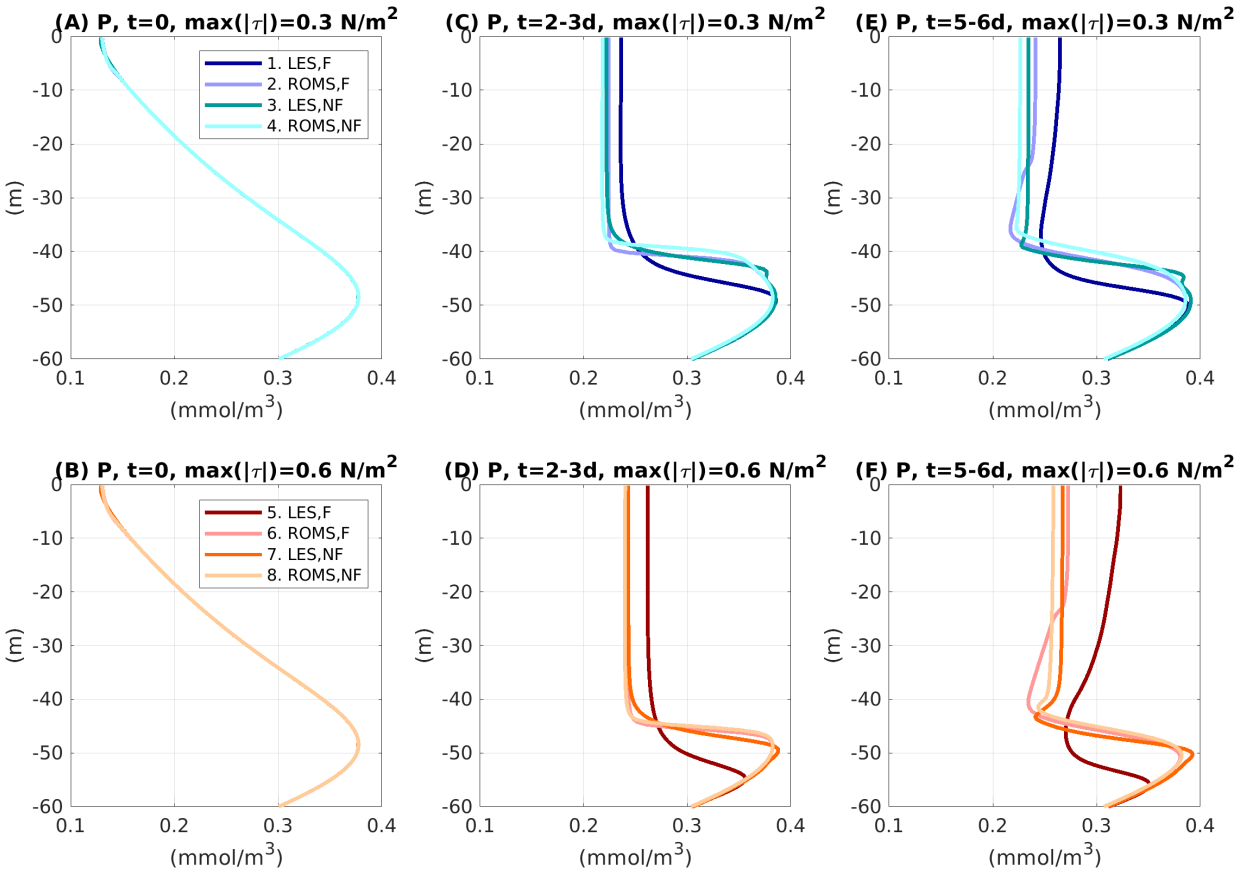

Figure 2: Horizontally-averaged vertical profiles of phytoplankton $\langle P \rangle_{x,y}$ averaged over several time periods during the evolution of the idealized storm life cycle, including $t = 0$ days (the initial time), $t = 2 - 3$ days (during the storm), and $t = 5 - 6$ days (after the storm). The results are also grouped by the magnitude of the wind stress, with the results from four simulations forced by the weaker wind scenario in the top row and results from four simulations forced by the stronger wind scenario in the bottom row. In the caption, F indicates the frontal zone, and NF indicates no front. LES indicates a large eddy simulation, whereas ROMS indicates a simulation with the column model. Only the top 60 m is shown to highlight the surface properties of interest.

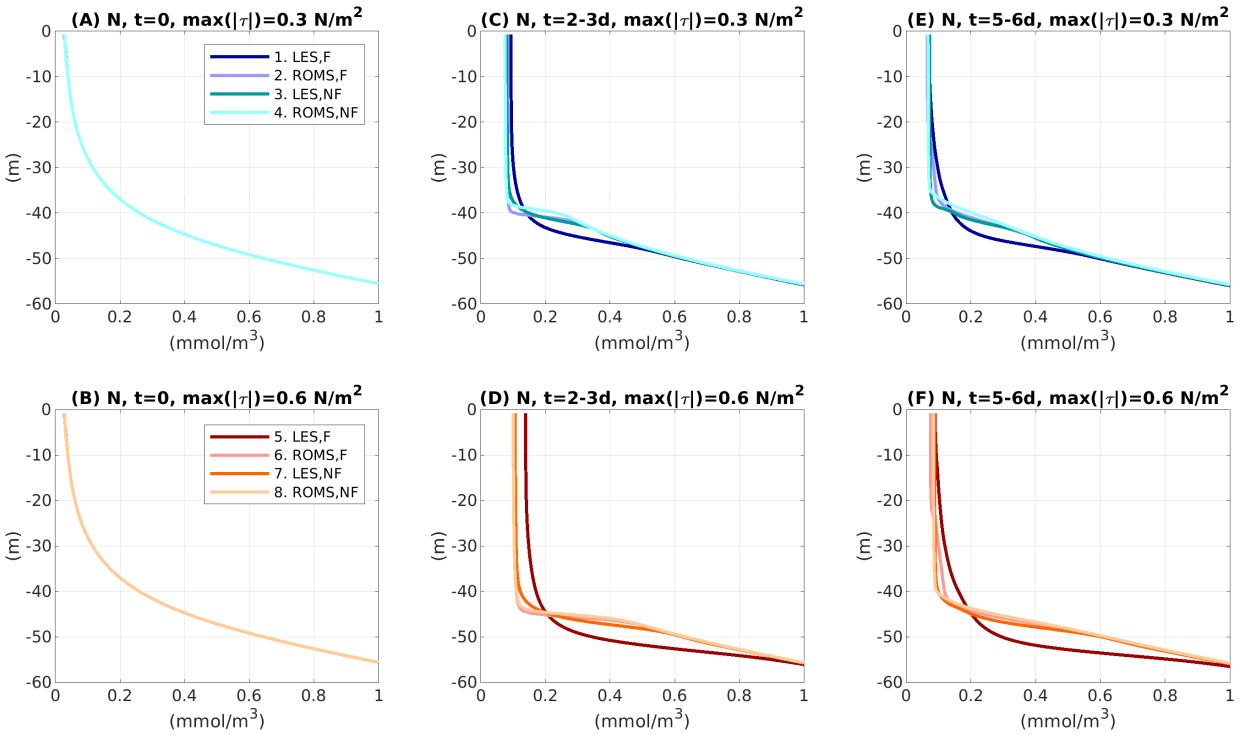

Figure 3: As in Fig. 2, but horizontally-averaged vertical profiles of nutrient $\langle N \rangle_{x,y}$.

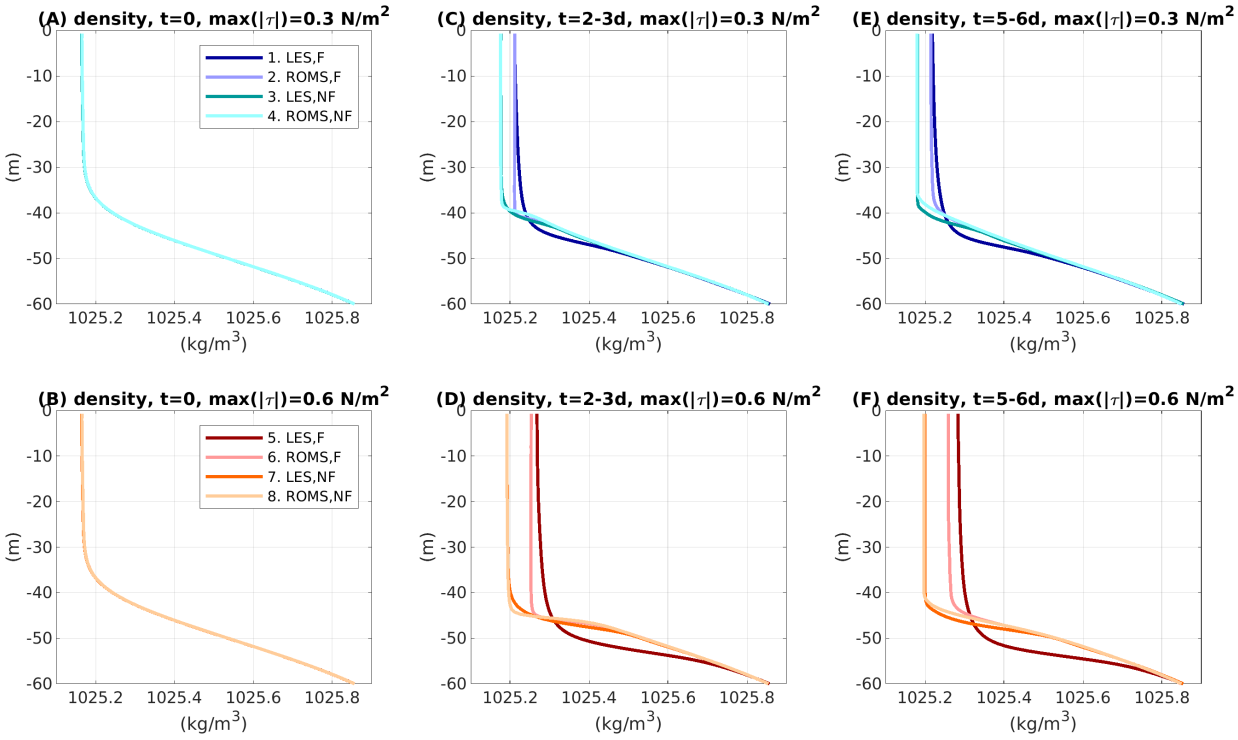

Figure 4: As in Fig. 2, but horizontally-averaged vertical profiles of density $\langle \rho \rangle_{x,y}$.

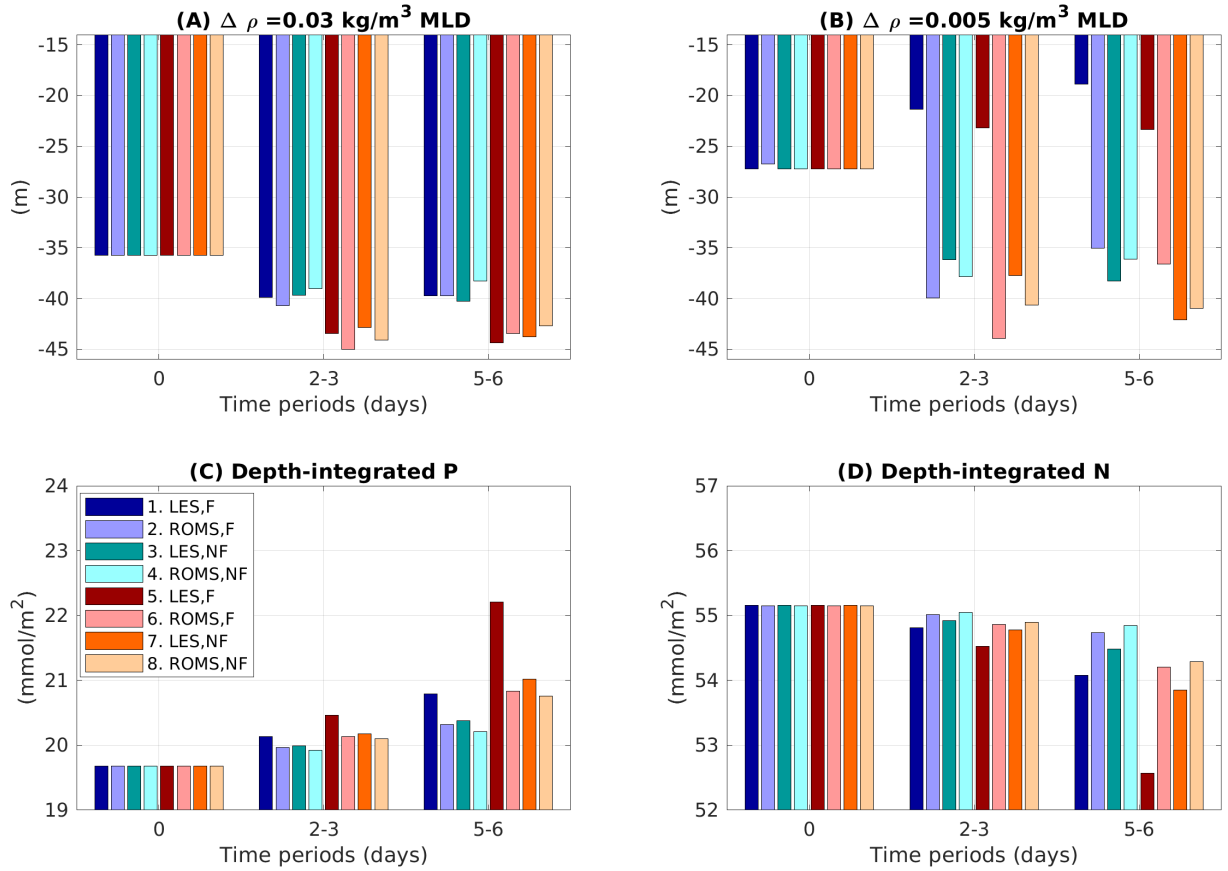

Figure 5: Two mixed layer depths based on different density thresholds relative to the density at the surface in (a), (b) and column integrals of phytoplankton $\langle P \rangle_{x,y}$ (c) and nutrient $\langle N \rangle_{x,y}$ (d). All four variables are presented as averages over three different time windows. Blue bars represent the four simulations forced with the weaker stress max $|\boldsymbol{\tau}| = 0.3$ N/m^2, and red bars represent the four simulations forced with stronger stress max $|\boldsymbol{\tau}| = 0.6$ N/m^2. The storm forcing occurs from days 0-3, as shown in Fig. 1 here. The caption labels are as in Figs. 2-4, that is F indicates the frontal zone, and NF indicates no frontal zone. LES indicates a large eddy simulation, whereas ROMS indicates a column model simulation.

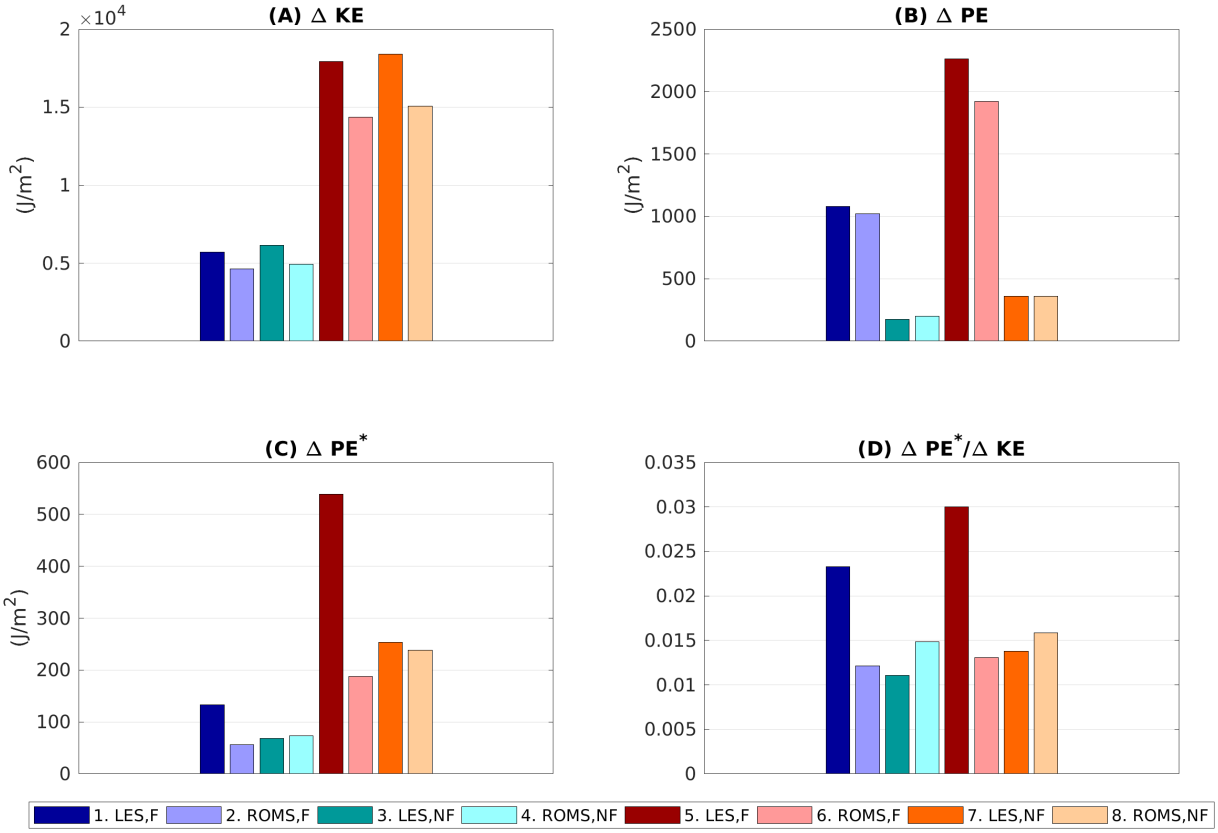

Figure 6: As in Fig. 5, but (a) shows the time-integrated wind work, $\Delta KE = \int_0^t \boldsymbol{\tau} \cdot \mathbf{u}_h(z = 0)\, ds$ where s is a dummy time integration variable, and (b) shows the change in depth-integrated potential energy $\Delta PE = \Delta \int_{z=-D}^{0} \rho g(z + H)\, dz$, and the Δ indicates that the difference is taken between an average over $t = 5 - 6$ days and $t = 0$ days. The domain depth $H = 80$ m. (c) shows the residual change in potential energy due to vertical mixing ΔPE^*, which approximately excludes the effect of the density increase in the surface mixed layer due to EBF and B_A (see the main manuscript). Estimates of the efficiency of the wind forcing ΔKE at driving increases in ΔPE^* are shown in (d).

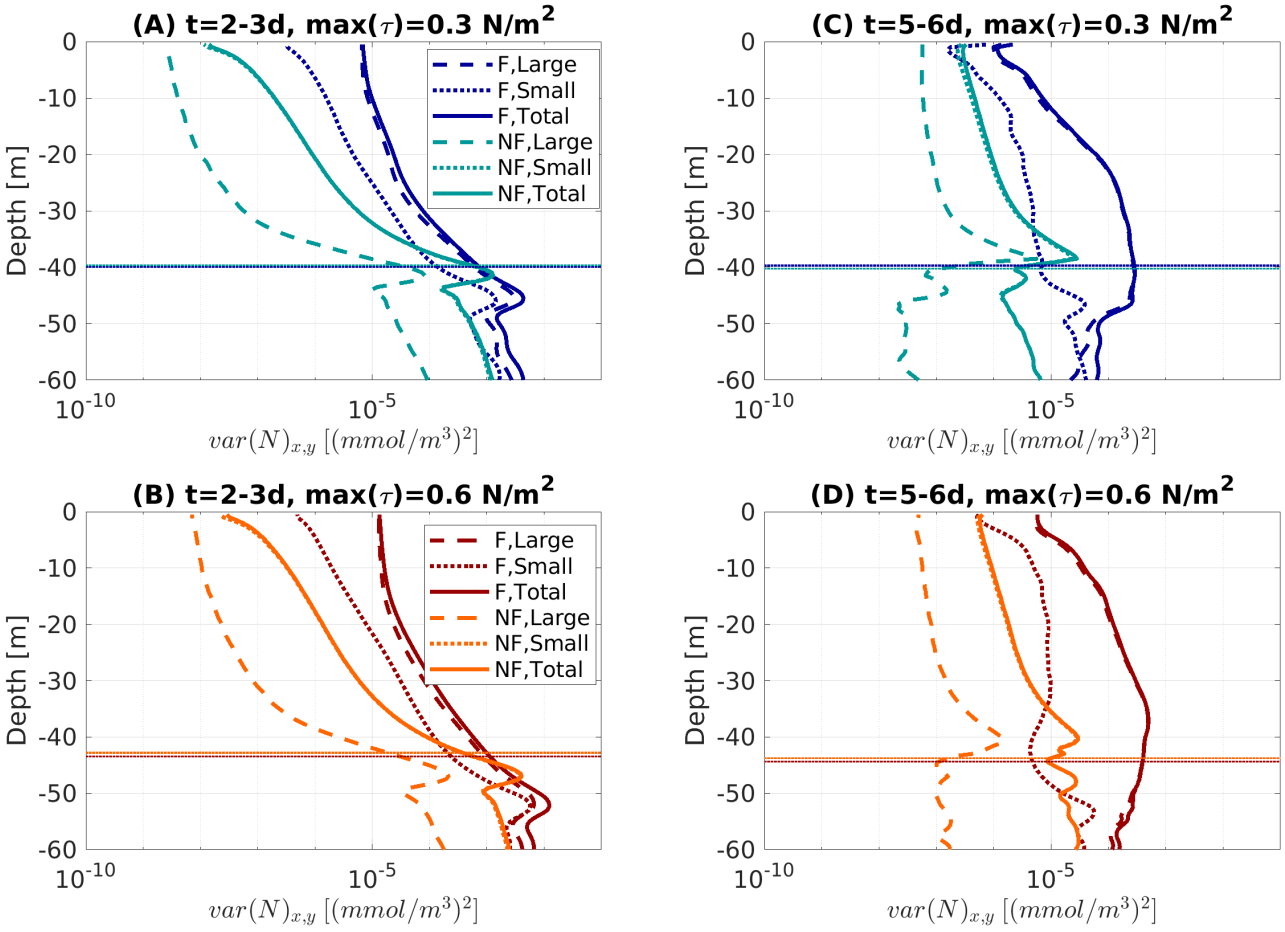

Figure 7: Multi-scale vertical profiles of nutrient variance $var(N)_{x,y}(z)$ from the four LES experiments, both during (a)-(b) and after the storm (c)-(d). Results from the two scenarios with a maximum stress $|\boldsymbol{\tau}| = 0.3$ N/m^2 are shown in (a) and (c), whereas results from the scenario with a maximum stress $|\boldsymbol{\tau}| = 0.6$ N/m^2 are shown in (b) and (d). In the caption, F indicates the frontal zone, and NF indicates no front. Large scales (dashed lines), that is wavelengths between 0.15 and 2 km, are separated from small scales (dotted lines), that is wavelengths < 0.15 km, using the spectra. The mixed layer depths H_{ML} defined by the $\Delta\rho = 0.03$ kg/m^3 method are plotted as thin horizontal dotted lines. Only the top 60 m is shown to highlight the surface properties of interest.

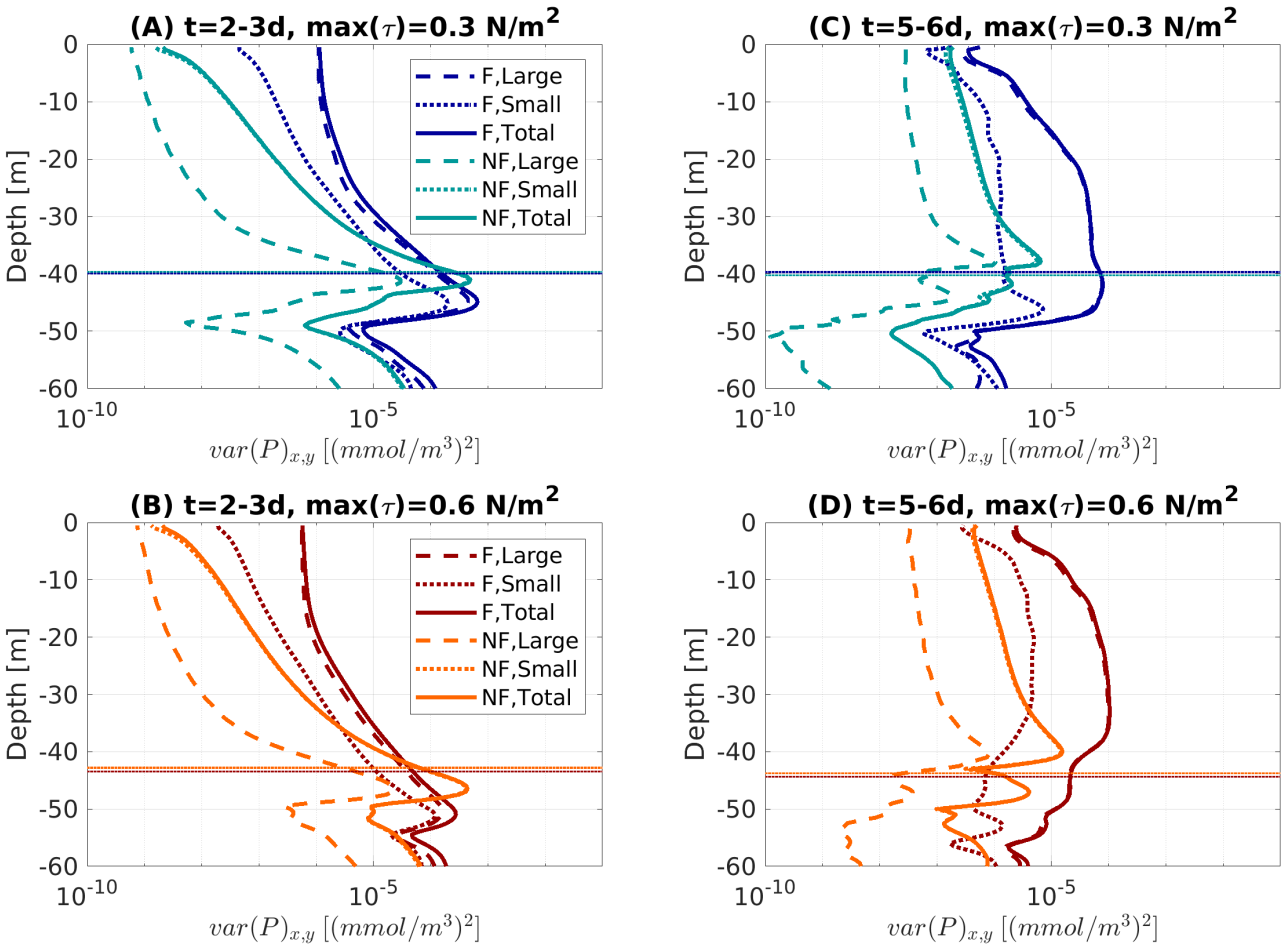

Figure 8: As in Fig. 7, but vertical profiles of multi-scale phytoplankton variance $var(P)_{x,y}(z)$.

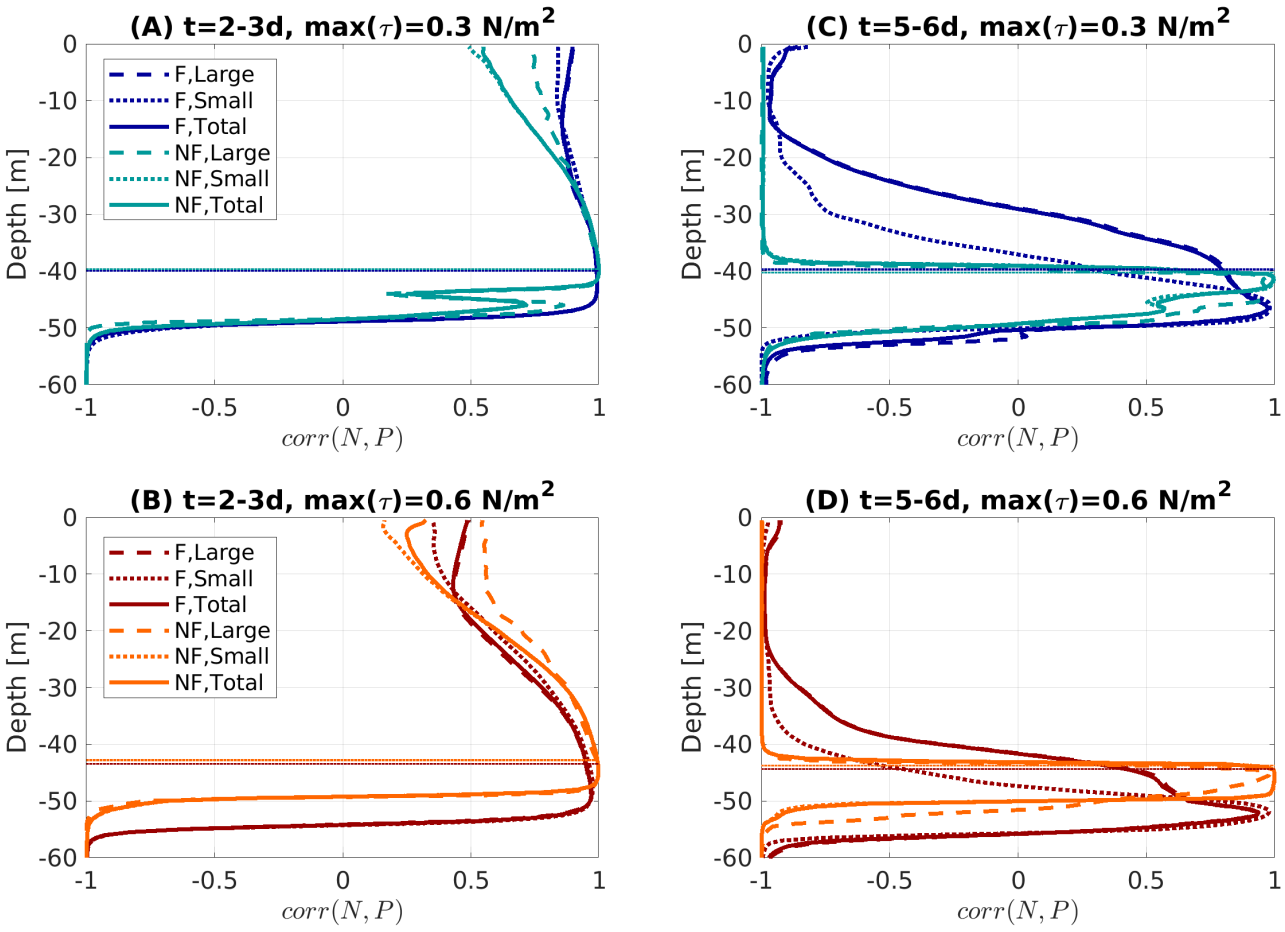

Figure 9: Similar to Fig. 7, but multi-scale Pearson's correlation between nutrient and phytoplankton. That is, $corr(N,P) = cov_{x,y}(N,P)/\sqrt{var_{x,y}(N)_{x,y}var_{x,y}(P)}$ where $cov_{x,y}$ is the covariance. The multi-scale covariances and variances are computed by integrating both the co-spectra and power spectra over three different ranges of wavelengths: both are integrated over submesoscale wavelengths greater than 0.15 km to produce the correlations labeled "large"; both are integrated over turbulent scale wavelengths less than 0.15 km to produce the results labeled "small"; and, finally, both are integrated over all resolved scales to produce the results labeled "total".

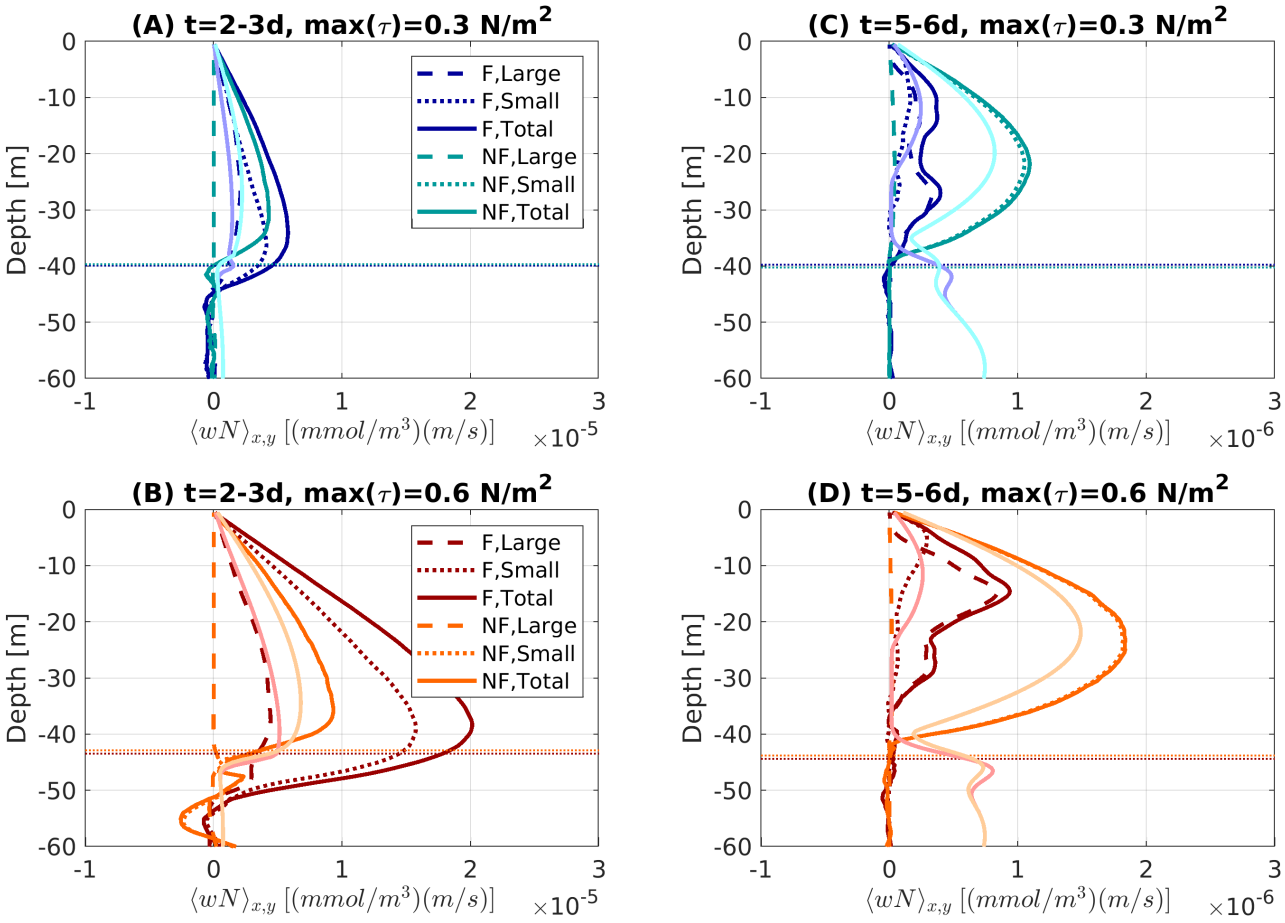

Figure 10: Similar to Fig. 7, but multi-scale vertical nutrient fluxes $\langle wN \rangle_{x,y}(z)$ from the four LES experiments, both during (a)-(b) and after the storm (c)-(d). Results from the two scenarios with a maximum stress $|\boldsymbol{\tau}| = 0.3$ N/m^2 are shown in (a) and (c), whereas results from the scenario with a maximum stress $|\boldsymbol{\tau}| = 0.6$ N/m^2 are shown in (b) and (d). In the caption, F indicates the frontal zone, and NF indicates no front. Large scales (dashed lines), that is wavelengths between 0.15 and 2 km, are separated from small scales (dotted lines), that is wavelengths < 0.15 km, using the cospectra. The mixed layer depths MLD_3 defined by the $\Delta\rho = 0.03$ kg/m^3 method are plotted as thin horizontal dotted lines. The total diffusive flux from the ROMS experiments is also shown for comparison; the line colors are as in Figs. 5.

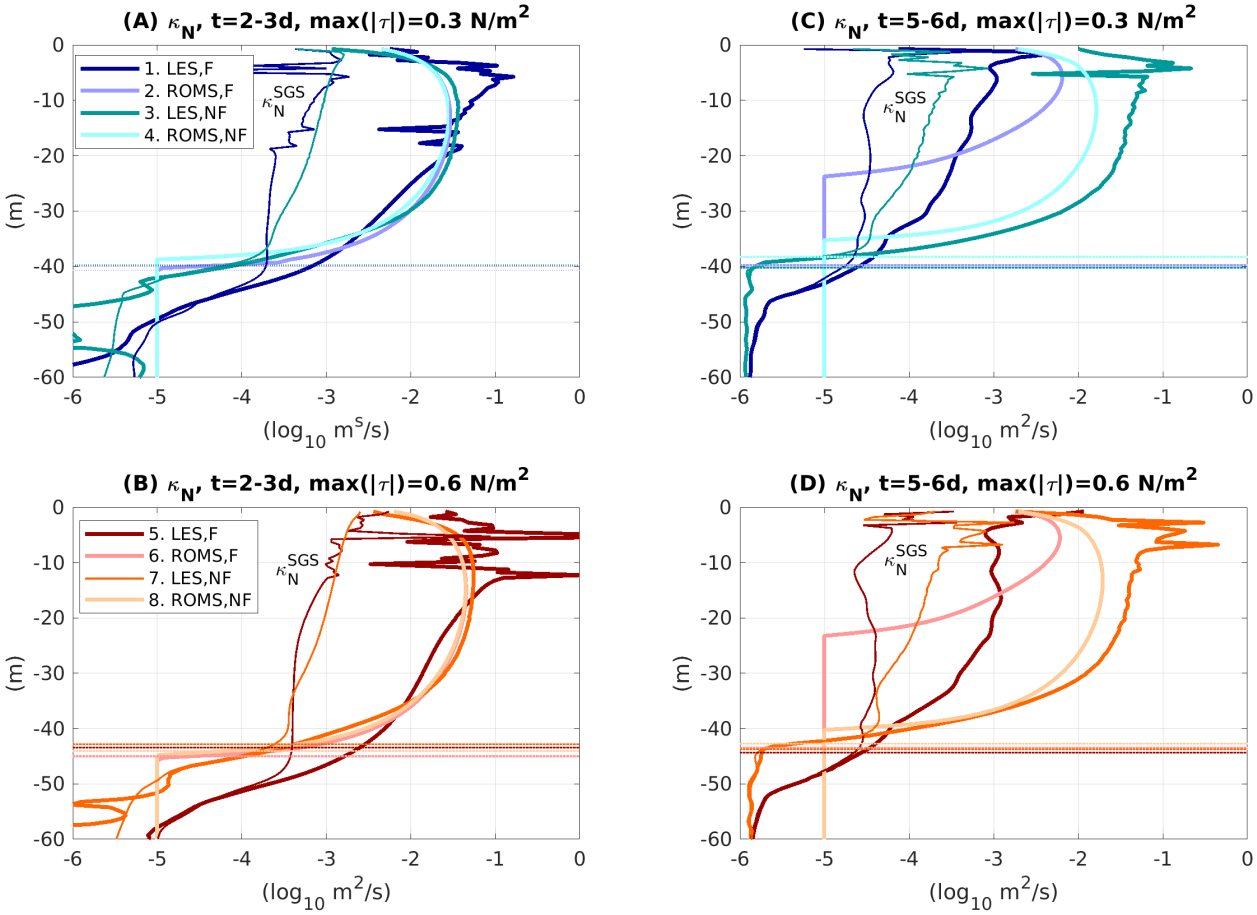

Figure 11: As in Fig. 2, but horizontally-averaged vertical profiles of the vertical diffusivity of nutrient κ_N, which is calculated as $\kappa_N = [\langle \kappa_{SGS}(\partial N/\partial z)\rangle_{x,y} - \langle wN\rangle_{x,y})/(\partial\langle N\rangle_{x,y}/\partial z)]$ in the LES and $\kappa_N = \kappa_T$ is an output of the KPP parameterization in the ROMS model. The subgrid scale contributions are plotted seperately as thin lines in the LES scenarios, that is $\kappa_N^{SGS} = [\langle \kappa_{SGS}(\partial N/\partial z)\rangle_{x,y})/(\partial\langle N\rangle_{x,y}/\partial z)]$. The mixed layer depths MLD_3 defined by the $\Delta\rho = 0.03$ kg/m^3 method are plotted as thin horizontal dotted lines.

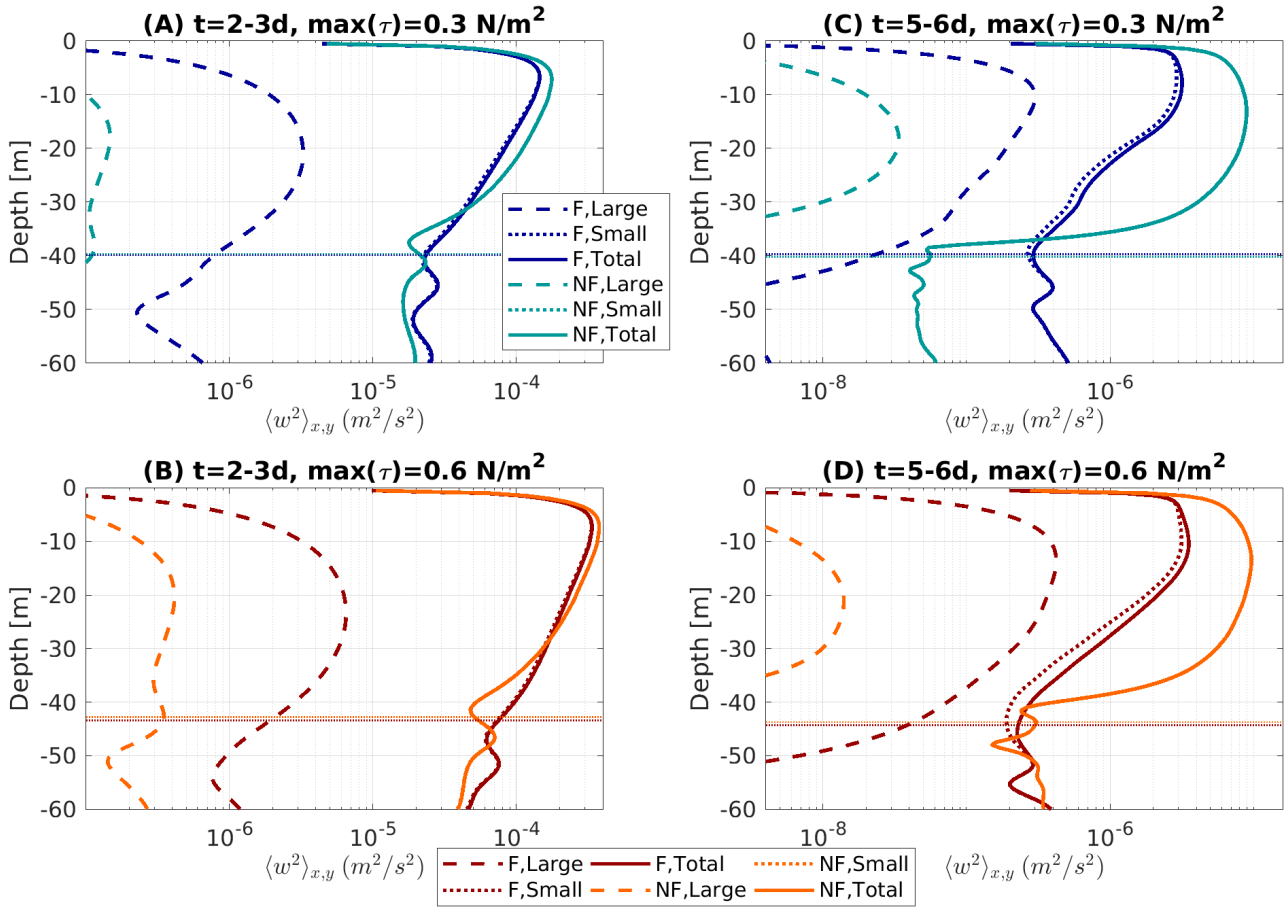

Figure 12: As in Fig. 7, but vertical profiles of multi-scale vertical velocity variance $var(w)_{x,y}(z)$.

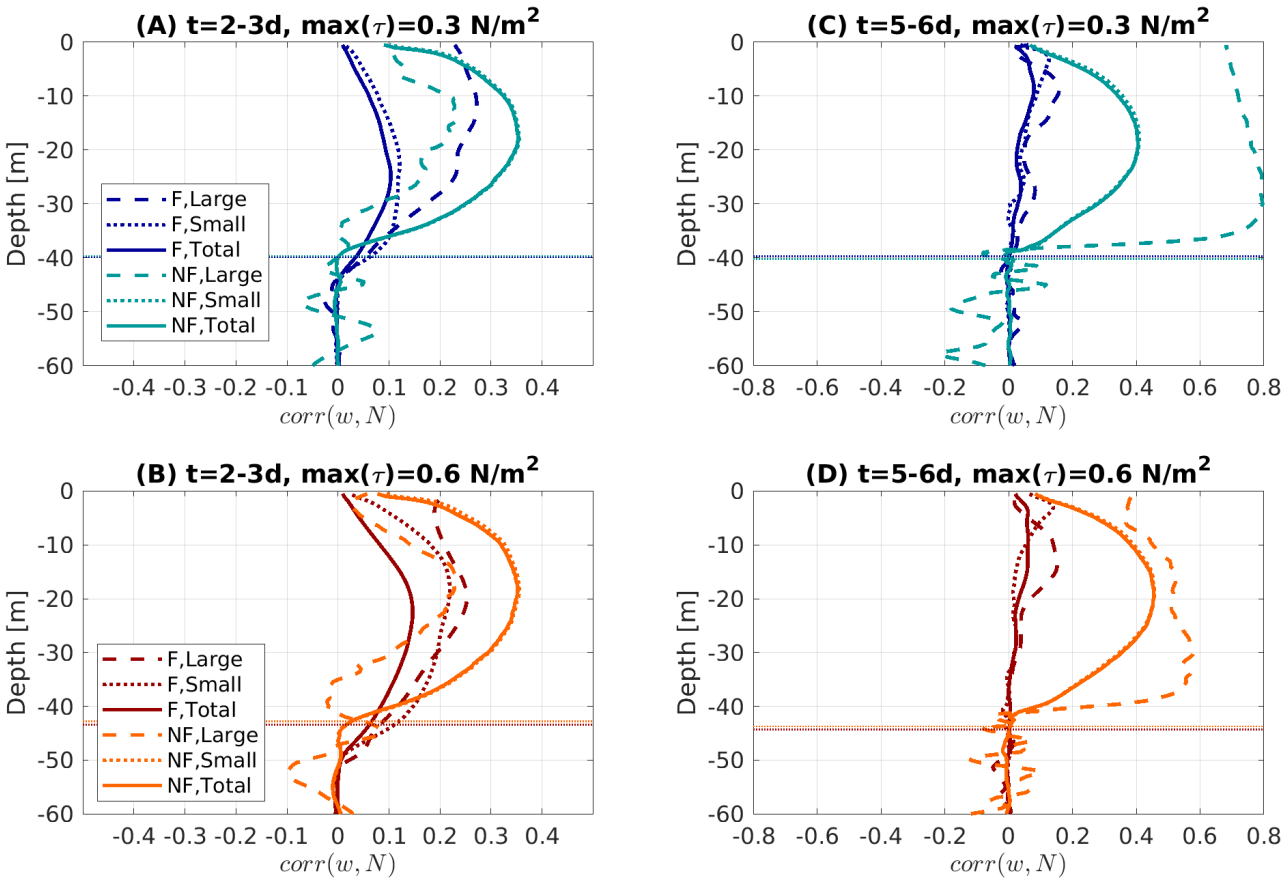

Figure 13: Similar to Fig. 9, but multi-scale Pearson's correlation between nutrient and vertical velocity. That is, $corr(w, N) = cov_{x,y}(w, N)/\sqrt{var_{x,y}(w)_{x,y} var_{x,y}(N)}$.